Modeling and Analysis of Thermal Effects in Optical Networks-on-Chip

Yaoyao Ye[1], Jiang Xu[1], Xiaowen Wu[1], Wei Zhang[2], Xuan Wang[1], Mahdi Nikdast[1], Zhehui Wang[1], Weichen Liu[1]
[1]ECE, Hong Kong University of Science and Technology, Hong Kong
[2]School of Computer Engineering, Nanyang Technological University, Singapore
Email: jiang.xu@ust.hk, zhangwei@ntu.edu.sg

***Abstract*—The performance of multiprocessor systems, such as chip multiprocessors (CMPs), is determined not only by the performance of their processors, but also by how efficiently they collaborate with one another. It is the communication architectures which determine the collaboration efficiency on the hardware side. Optical networks-on-chip (ONoCs) are emerging communication architectures that can potentially offer ultra-high communication bandwidth and low latency to multiprocessor systems. Thermal sensitivity is an intrinsic characteristic of photonic devices used by ONoCs as well as a potential issue. For the first time, this paper systematically modeled and quantitatively analyzed the thermal effects in ONoCs and their impacts. We presented an analytical ONoC thermal model, and show that on-chip temperature fluctuations can dramatically reduce the worst-case ONoC power efficiency. For instance, the power efficiency of an ONoC will drop to about $5pJ/bit$ when chip temperature reaches 85^oC. We revealed three important factors regarding ONoC power efficiency under temperature variations, and found the optimal initial device conditions to minimize thermal impacts. The impacts of the thermal effects on the ONoC power consumption under different chip temperatures, device characteristics, and ONoC configurations are quantitatively analyzed. The findings in this paper can help support the further development of this emerging technology.**

***Keywords*—optical network-on-chip; thermal effect; temperature sensitivity;**

I. Introduction

With the burgeoning complexity of multiprocessor systems, such as chip multiprocessors (CMPs), tens and even hundreds of processor cores are required to be integrated on a single chip. The performance of multiprocessor systems is determined not only by the performance of their processors, but also by how efficiently they collaborate with one another. It is the communication architectures which determine the collaboration efficiency on the hardware side. An efficient on-chip communication architecture can help fully utilize the computation resources offered by multiple processor cores on a CMP. On-chip communication architectures have gradually moved to network-on-chip (NoC) to alleviate the poor scalability, limited bandwidth, and high power consumption in traditional interconnection networks [1], [2].

As semiconductor technologies continually shrink feature sizes and new applications demand even more on-chip communications, conventional metallic interconnects are becoming the bottleneck of NoCs. As emerging communication architectures, optical networks-on-chip (ONoCs) are based on photonic technologies, and can potentially offer ultra-high communication bandwidth, low latency, and high energy efficiency to multiprocessor systems. Recent developments in nanoscale silicon photonic devices substantially improve the feasibility of ONoCs [3], and different ONoC architectures have been developed based on optical waveguides and microresonators [4]–[9].

Thermal sensitivity is an intrinsic characteristic of photonic devices, and is a potential issue in ONoC designs. On-chip temperature variations can affect the physical properties of photonic devices and change their operating points. Such thermal effects can potentially cause ONoC performance degradation and even functional failure under large chip temperature fluctuations. Chip temperature can fluctuate temporally as well as spatially. It can rise quickly from room temperature after a cold start, and vary by more than 30^oC across a steady-state chip under typical operating conditions [10]. An ONoC thermal model is required to fully understand these challenges and help the further development of this emerging technology.

For the first time, this paper systematically modeled the thermal effects in ONoCs and discovered the optimal device settings to minimize such impacts. Our analysis shows that the worst-case power efficiency of ONoCs would degrade significantly under chip temperature fluctuations. For instance, if the chip temperature varies spatially between 55^oC and 85^oC, the worst-case power efficiency of an ONoC with three switching stages on its links will degrade from $1.8pJ/bit$ to about $5pJ/bit$. Based on the ONoC thermal model, we reveal three important factors affecting ONoC power efficiency under temperature variations, including the initial photonic device conditions, the number of switching stages in an ONoC architecture, and the bandwidth of each switching element in the ONoC. By finding the optimal device initial conditions, we show that the worst-case power efficiency can be improved by about 32%.

The rest of paper is organized as follows. Section II presents the ONoC thermal model based on the detailed analysis of the thermal effects on transmitters, switching elements, optical waveguides, and receivers in ONoC architectures. Section III quantitatively analyzes the thermal effects in ONoCs under different configurations. Section IV draws the conclusions of the paper.

978-0-7695-4447-2/11 $26.00 © 2011 IEEE
DOI 10.1109/ISVLSI.2011.38

II. ONoC Thermal Model

Most ONoC architectures employ photonic devices which can be integrated with existing CMOS-based processor cores either through CMOS-compatible fabrication processes or bonding technologies. Despite of the architecture diversity, an optical link in ONoCs is usually composed of an optical transmitter, an optical path, and an optical receiver (Figure 1). The optical transmitter can convert electrical signals into optical signals by directly modulating the driving current of a VCSEL (vertical cavity surface emitting laser) [11] or using an optical modulator, such as a microresonator, to indirectly modulate the laser outputted by a VCSEL or an off-chip laser source. The optical receiver uses photodetectors to convert optical signals into electrical signals used by processors or memories in electronic domains. On the optical path between the transmitter and receiver, multiple switching elements switch optical signals in stages onto a series of optical waveguides until reaching their destination. Microresonator-based add-drop filters have been widely used as the switching element to perform the switching function in ONoCs [12]–[15].

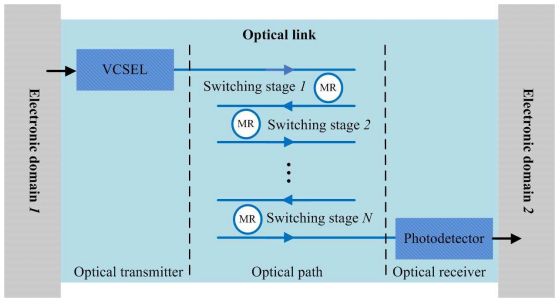

Fig. 1. An overview of the optical link in ONoCs connecting two electronic domains

Chip temperature varies spatially across the chip die because of the non-uniform power densities as well as the limited thermal conductivity of the die and packaging materials. For example, in Intel Itanium processor which is under stringent thermal management, while some part of the chip can be maintained at a relatively low temperature of 60^oC, the other part of chip can still reach about 88^oC [16]. Silicon-based photonic devices can provide better compatibility to ONoCs, but temperature fluctuations can affect the refractive index of silicon [17], and hence affect the operating point of photonic devices. In the following sessions, we will systematically develop a thermal model for ONoCs.

A. Thermal Sensitivity of Optical Transmitters

Optical transmitters convert electrical signals into optical signals by either directly modulating the driving currents of VCSELs or using an optical modulator, such as a microresonator, to indirectly modulate the lasers outputted by VCSELs or off-chip laser sources. Based on the rapid technology advancements in recent years, VCSELs are chosen by many ONoC architectures to fully integrate ONoCs on CMPs. The characteristics of VCSELs are sensitive to temperature variations. As in Equation (1), the emission wavelength λ_{VCSEL} is determined by the cavity resonance, where $n_{average}$ is the spatially averaged refractive index of the resonator, l_{VCSEL} is the length of the inner cavity, and m_{VCSEL} is the resonance order [18]. The temperature dependent shift of VCSEL emission wavelength is mainly governed by the change of $n_{average}$, which is dependent on the material composition of its Bragg reflectors and inner cavity.

$$l_{VCSEL} \cdot n_{average} = m_{VCSEL} \cdot \lambda_{VCSEL}/2 \tag{1}$$

For VCSELs in the emission wavelength range 800-1000nm, the temperature dependent wavelength shift is typically found to be 0.07nm per ^oC, and the shift of the peak material gain wavelength is about 0.32nm per ^oC [18]. The investigation of a 1300nm VCSEL shows a similar result [19]. Because of the different shift of cavity resonance and peak gain, a mutual shift of the lasing mode and gain spectrum occurs when temperature changes. The misalignment causes the threshold current I_{th} of VCSEL to increase with temperature T following an approximate parabolic shaped curve shown by Equation (2), where α is the minimum threshold current, β is a coefficient related to the gain properties, and T_{th} is the temperature at which the cavity resonance is spectrally aligned with the peak gain [20].

$$I_{th} = \alpha + \beta(T - T_{th})^2 \tag{2}$$

If the driving current is above the threshold, the output power will increase approximately linearly with the driving current. Slope efficiency is the incremental increase in output power for an incremental increase in driving current. The slope efficiency decreases approximately linearly with an increasing temperature, and can be expressed by Equation (3), where ε is the slope efficiency at 0^oC, and γ is a positive coefficient. For the VCSEL demonstrated in [11], the slope efficiency decreases from $0.36mW/mA$ to $0.23mW/mA$ when the temperature increases from room temperature to 80^oC. Meanwhile, the maximum emission power decreases from $4mW$ to $1.5mW$ correspondingly.

$$s = \varepsilon - \gamma \cdot T \tag{3}$$

B. Thermal Sensitivity of Switching Elements

On the optical path between the transmitter and receiver, multiple switching elements switch optical signals in stages onto a series of optical waveguides until reaching their destination. We use a simplified model of a ring-based microresonator to perform the switching function in Figure 1. The peak resonant wavelength λ_{MR} of a microresonator obeys the relationship in Equation (4), where l_{MR} is the one-round path length of the ring, m_{MR} is an integer indicating the order of the resonance, and n_{eff} is the effective index of the waveguide mode involved in the resonance.

$$l_{MR} \cdot n_{eff} = m_{MR} \cdot \lambda_{MR} \tag{4}$$

With a constant l_{MR} and m_{MR}, the peak resonant wavelength λ_{MR} will change in proportion with n_{eff}. Since n_{eff}

changes with the temperature, the peak resonant wavelength will also vary with the temperature. Both theoretical analysis and experiment results confirm a linear relationship between the shift of resonant wavelength and temperature. The linear relationship can be expressed as Equation (5), where ρ_{MR} is defined as the microresonator temperature dependent wavelength shift, λ_{MR_0} is the resonant wavelength at an initial temperature, σ_{eff} is the thermo-optic coefficient (dn/dT) of the effective index, and n_g is the group index of the waveguide [21]. Experiments show that microresonators shift the resonant wavelength about 50pm per ^oC [22].

$$\rho_{MR} = \frac{\lambda_{MR\_0}}{n_g} \cdot \sigma_{eff} \tag{5}$$

An ideal lossless microresonator would confine light indefinitely, but intrinsic loss always exists in any physical implementation of cavities. The deviation from the ideal condition is defined by the quality factor Q, which is proportional to the confinement time of the cavity. The total quality factor of a ring-based microresonator used in Figure 1 is defined by Equation (6), where λ_{MR} is the resonant wavelength, 2δ is the 3-dB bandwidth of the drop-port power transfer spectrum, κ_e^2 is the fraction of power coupling between the input waveguide and the ring, κ_d^2 is the fraction of power coupling between the drop waveguide and the ring, and κ_p^2 is the power loss per round-trip of the ring [23]. Microresonators with Q ranging from 1500 to 100,000 have been demonstrated using different structures [24].

$$Q = \frac{\lambda_{MR}}{2\delta} = \frac{2\pi n_g l_{MR}}{\lambda_{MR}(\kappa_e^2 + \kappa_d^2 + \kappa_p^2)} \tag{6}$$

Microresonators have a Lorentzian power transfer function which is peaked at the resonant wavelength λ_{MR}. For optical signals carried on wavelength λ_s, the drop-port power transfer can be expressed as Equation (7) [25]. When $\kappa_d^2 + \kappa_e^2 \gg \kappa_p^2$, nearly full power transfer can be achieved at the peak resonance point, and the microresonator will exhibit a low insertion loss. Physical implementations show that the insertion loss of a microresonator can be practically lowered to $0.5dB$ [26].

$$\frac{P_{drop}}{P_{in}} = (\frac{2\kappa_e\kappa_d}{\kappa_e^2 + \kappa_d^2 + \kappa_p^2})^2 \cdot \frac{\delta^2}{(\lambda_s - \lambda_{MR})^2 + \delta^2} \tag{7}$$

According to Equation (7), a deviation from the peak resonant wavelength would result in more power loss at the drop port especially for a high-Q microresonator. For a microresonator at the 1550nm wavelength range, if the quality factor Q is on the order of 10^4, a 10^oC temperature change would make the power spectrum shift about *0.5nm* and result in a power loss variation of about *16dB* for optical signals carried by 1550nm wavelength. For ONoCs requiring multiple switching stages on each optical link, the problem can become even more serious as multiple switching elements could reduce the optical signal strength significantly (Figure 1).

C. Thermal Sensitivity of Optical Waveguides

ONoCs use optical waveguides to connect transmitters, switching elements, and receivers together to form optical links. Silicon-based waveguides can be fabricated on silicon-on-isolator (SOI) substrate with a silicon slab on top of a buried oxide (BOX) layer which prevents optical mode from leaking to the substrate. The cross-section of a single-mode waveguide can be designed to be $510nm \times 226nm$ with minimum propagation loss and group velocity dispersion [27]. The silicon core of a waveguide has negligible absorption of energy and waveguide propagation loss is dominated by the sidewall roughness scattering.

$$L_{WG} = \frac{4\epsilon^2 k_0^2 h}{\beta} \cdot \frac{E_s^2}{\int E^2 dx} \cdot \phi^2 \tag{8}$$

Propagation loss in a straight optical waveguide can be estimated by Equation (8), where ϵ is a parameter regarding the interface roughness, k_0 is the free space wavenumber, β is the modal propagation constant, h is the transverse propagation constant in the waveguide core, ϕ is the refractive index difference between the waveguide core and cladding materials, and $E_s^2 / \int E^2 dx$ is the normalized electric field intensity at the waveguide core/cladding interface [28].

$$L_{WG} = L_{WG\_0} \cdot (1 + \frac{\sigma_c - \sigma_d}{\phi} \cdot \Delta T + \frac{(\sigma_c - \sigma_d)^2}{3\phi^2} \cdot (\Delta T)^2) \tag{9}$$

As shown in Equation (8), the waveguide propagation loss is proportional to the refractive index difference between the core and cladding, and because of the different thermo-optic coefficients (dn/dT) of the core and cladding materials, the propagation loss will also change with operating temperatures as a result of thermo-optic effect. Assume that the waveguide temperature increases by ΔT uniformly along the direction of light propagation, the corresponding variation of the waveguide propagation loss is expressed in Equation (9), where L_{WG_0} is the propagation loss at room temperature. σ_c and σ_d are defined as the thermo-optic coefficients (dn/dT) of the waveguide core and cladding materials respectively. For an optical waveguide with a Si core and SiO_2 cladding, the refractive index difference ϕ is approximately equal to 2. Based on Equation (9), the propagation loss variation on a Si/SiO_2 waveguide is about 0.22% for a 30^oC temperature change. The thermal-related variation of waveguide propagation loss is less sensitive to temperature compared to the insertion loss of a high-Q switching element.

D. Thermal Sensitivity of Optical Receivers

Optical receivers use photodetectors to convert optical signals into electrical signals used by processors or memories in electronic domains. Most photodetector designs use Ge as the absorbing material because of the high absorption coefficient of Ge in the near infrared spectrum as well as its compatibility with CMOS fabrication processes. By monolithically integrating Ge-based photodetector with high-speed TIA-LA circuits, a 10Gbps optical receiver can achieve a sensitivity of $-14.2dBm$ with a bit error rate (BER) of 10^{-12} in the 1550nm wavelength range [29]. A major concern for the temperature-dependent behaviors of Ge-based photodetectors

is the potential excessive dark current under high operating temperatures. Studies show that the dark current of a $10\mu m \times 10\mu m$ Ge-on-SOI photodetector increases from $20nA$ to $192nA$ when temperature change from room temperature to 86^oC, while the receiver sensitivity does not have obvious change [30], [31]. Although the dark current of a photodetector increases with temperature, it is still sufficiently low (generally less than $1\mu A$) so as not to degrade the receiver performance even under a high operating temperature. Based on above observations, we assume that the sensitivity of the optical receiver does not change with the operating temperature in our ONoC thermal model.

E. ONoC Thermal Model

To ensure ONoCs function properly, a necessary condition is that the optical signal power received by the receiver of an optical link should not be lower than the receiver sensitivity. This condition can be modeled by Equation (10), where P_{TX} is the output power of the optical transmitter on a link, L_{SW} is the optical power loss due to the switching elements, L_{WG} is the optical power loss due to the waveguides, and S_{RX} is the sensitivity of the receiver.

$$P_{TX} - L_{SW} - L_{WG} \geq S_{RX} \tag{10}$$

As analyzed earlier, the output power of VCSELs degrades at higher operating temperatures. Assuming that the VCSEL is driven by current I which is above the threshold but before the point where the output power starts to decrease with current, we can express P_{TX} by Equation (11), where $T_{VCSEL} \in [T_{min}, T_{max}]$ is the VCSEL operating temperature, and α, β, ε, and γ are positive parameters we defined in the earlier section.

$$P_{TX} = (I - \alpha - \beta(T_{VCSEL} - T_{th})^2)(\varepsilon - \gamma \cdot T_{VCSEL}) \tag{11}$$

The spatial temperature fluctuations in ONoCs will result in mismatches between the VCSELs lasing wavelength and the resonant wavelength of switching elements. The lasing wavelength of VCSELs red-shift approximately linearly with temperature, which can be calculated by Equation (12). λ_{VCSEL_min} is the VCSEL lasing wavelength at temperature T_{min}, and ρ_{VCSEL} is defined as the VCSEL temperature dependent wavelength shift.

$$\lambda_{VCSEL} = \lambda_{VCSEL\_min} + \rho_{VCSEL}(T_{VCSEL} - T_{min}) \tag{12}$$

The resonant wavelengths of microresonators also red-shift approximately linearly with increasing temperatures. For a microresonator working at temperature $T_{MR} \in [T_{min}, T_{max}]$, the resonant point is as in Equation (13), where λ_{MR_min} is the resonant wavelength at T_{min}.

$$\lambda_{MR} = \lambda_{MR\_min} + \rho_{MR}(T_{MR} - T_{min}) \tag{13}$$

Considering the thermal-induced wavelength mismatches on an optical link with N switching stages, the optical power loss due to the switching elements L_{SW} can be calculated by Equation (14). We assume that all the switching elements in the ONoC are identical and symmetrically coupled with a ring-waveguide coupling efficiency of κ^2. Microresonator at the i_{th} switching stage works at temperature T_{MR_i} ($T_{min} \leq T_{MR_i} \leq T_{max}$).

$$\begin{aligned} L_{SW} = \sum_{i=1}^{N} 10log((\frac{2\kappa^2 + \kappa_p^2}{2\kappa^2})^2 \cdot (1 + (\lambda_{VCSEL\_min} \\ +\rho_{VCSEL}(T_{VCSEL} - T_{min}) - \rho_{MR}(T_{MR_i} - T_{min}) \\ -\lambda_{MR\_min})^2/\delta^2)) \end{aligned} \tag{14}$$

Based on the above analysis, we can get the ONoC thermal model in Equation (15). The last term of the equation is the optical power loss due to the waveguides on the optical link. The thermal model shows that under a high power loss in the optical path caused by chip temperature fluctuations, more input power would be needed by the transmitter to guarantee enough optical power reaching the receiver. The thermal-induced optical power received at the end of an ONoC link can be calculated by the left side of Equation (15).

$$\begin{aligned} 10log((I - \alpha - \beta(T_{VCSEL} - T_{th})^2)(\varepsilon - \gamma \cdot T_{VCSEL})) \\ - \sum_{i=1}^{N} 10log((\frac{2\kappa^2 + \kappa_p^2}{2\kappa^2})^2 \cdot (1 + \delta^{-2}(\lambda_{VCSEL\_min} \\ +\rho_{VCSEL}(T_{VCSEL} - T_{min}) - \rho_{MR}(T_{MR_i} - T_{min}) \\ -\lambda_{MR\_min})^2)) - L_{WG} \geq S_{RX} \end{aligned} \tag{15}$$

A closer study of the thermal model reveals several thermal properties of ONoCs. First, the number of switching stages N in an optical link can dramatically change the thermal-induced power consumption. Second, initial device settings can affect the thermal-induced power consumption. Third, the 3-dB bandwidth of the switching elements is an important factor of the thermal-induced power consumption. High-Q microresonator based switching elements have narrow pass-bands and will be more sensitive to the thermo-optic effects as compared with those with wider passbands. A detailed quantitative analysis of those properties is presented in the next section.

III. Analysis of Thermal Effects in ONoCs

Based on the analytical ONoC thermal model, we found the optimal device settings for ONoCs and quantitatively analyzed the impacts of the thermal effects in the ONoC power consumption under different temperature ranges, device characteristics, and ONoC configurations. We assume the lasing wavelength of VCSELs at room temperature $T_0 = 25^oC$ is 1550nm and ρ_{VCSEL} is $0.09nm$ per ^oC. ρ_{MR} is assumed to be $0.06nm$ per ^oC. We assume the minimum chip temperature during operation is $T_{min} = 55^oC$. During the analysis, the minimum threshold current α of the VCSELs is assumed to be $2.4mA$ at $T_{th} = 40^oC$, with $\beta = 0.00075$, $\varepsilon = 0.403$ and $\gamma = 0.00217$ [11]. The waveguide loss is assumed to be $4.6dB$ including $3.4dB$ waveguide propagation loss for a path length of 20mm under room temperature [27].

Figure 2 shows the worst-case optical power reaching the receiver when the VCSEL driving current is $12mA$. We assume that the 3-dB bandwidth of the microresonators is $1.55nm$,

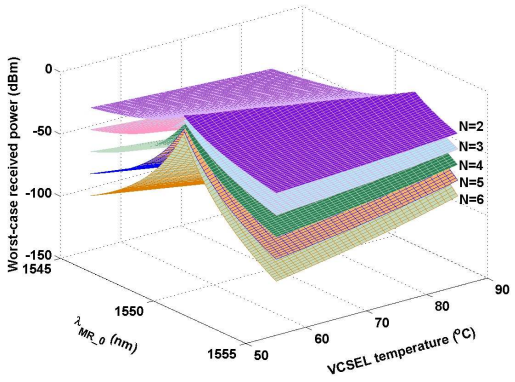

Fig. 2. The worst-case optical power received at the receiver, $2\delta = 1.55nm$, N is the number of switching stages.

and there are different numbers of the switching stages from 2 to 6. We find that because of the increasing loss on the optical link, the worst-case optical power decreases quickly as the number of switching stages increases. Figure 2 shows that the worst-case power loss under temperature variations has a upper bound, and indicates that the worst-case thermal-induced power loss can be minimized by properly setting the initial device conditions. We find that the lowest worst-case power loss can be reached by setting λ_{MR_0} and λ_{VCSEL_0} according to Equation (16), where T_0 is the room temperature. The equation shows that λ_{MR_0} should be moderately larger than λ_{VCSEL_0} if ρ_{VCSEL} is slightly larger than ρ_{MR}.

$$\lambda_{MR\_0} = \lambda_{VCSEL\_0} + \frac{(\rho_{VCSEL} - \rho_{MR})}{2} \cdot (T_{max} + T_{min} - 2T_0) \quad (16)$$

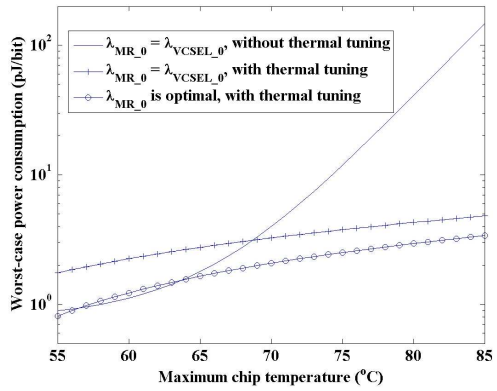

Fig. 3. The worst-case power consumption with optimal λ_{MR_0} and $\lambda_{MR\_0} = \lambda_{VCSEL\_0}$, $2\delta = 3.1nm$, $N = 3$.

Figure 3 shows that the worst-case power consumption when the switching elements are set to the optimal λ_{MR_0} or $\lambda_{MR\_0} = \lambda_{VCSEL\_0}$. By applying local thermal tuning of MRs with microheaters [32], the worst-case power consumption in an ONoC link with three switching stages can be reduced from $150pJ/bit$ to $5pJ/bit$. The optimal setting of λ_{MR_0} can further reduce the worst-case thermal-induced power loss and improve the power efficiency by 32% to $3.4pJ/bit$.

Figure 4 shows the worst-case power consumption with different 3-dB bandwidths under the optimal setting of λ_{MR_0} but without thermal tuning. It shows that the worst-case thermal-induced power consumption increases drastically with decreasing 3-dB bandwidth. These results show that high-Q microresonator-based switching elements are much more sensitive to temperature variations and the wavelength mismatches between the VCSEL and high-Q microresonators could cause an excessive optical power loss when no thermal tuning is assumed.

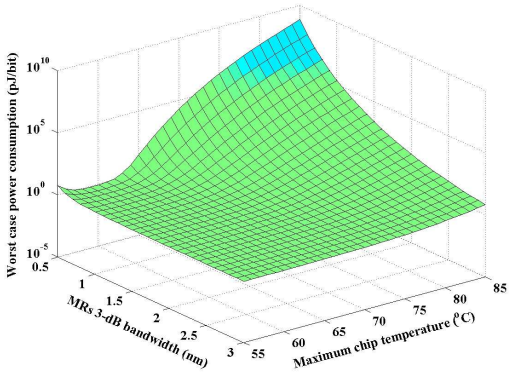

Fig. 4. The worst-case power consumption with different microresonator 3-dB bandwidths under optimal λ_{MR_0}, no thermal tuning is assumed, $N = 3$

Figure 5 shows the worst-case power consumption under different numbers of switching stage N. When $N = 4$, the worst-case power consumption with the optical λ_{MR_0} and thermal tuning is about $4.2pJ/bit$ if the maximum chip temperature is 85^oC. For ONoC links with a relatively large number of switching stages, for example $N = 6$, the worst-case power consumption is about $5.7pJ/bit$. When the number of switching stage N gets even larger, high maximum chip temperatures will cause significantly more impacts on ONoC power consumption. In this case, beside setting the device parameters according to Equation (16), it is also important to keep the worst-case number of switching stages in ONoCs as small as possible.

IV. Conclusions

We presented an analytical ONoC thermal model, and quantitatively analyzed the impacts of thermal effects on ONoC power consumption under different chip temperatures, device characteristics and ONoC configurations. Our analysis shows that the worst-case power efficiency of ONoCs degrades significantly under large on-chip temperature fluctuations. Based on the ONoC thermal model, we find that the worst-case power efficiency can be improved by about 32% by properly setting the device initial conditions. The number of

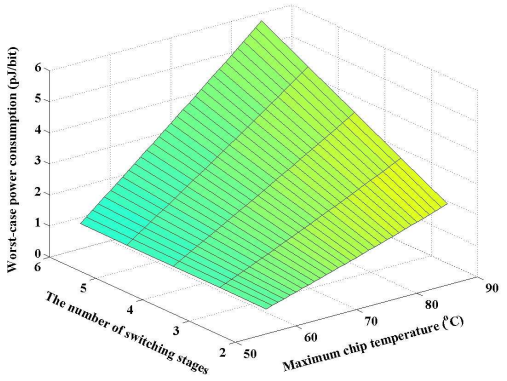

Fig. 5. The worst-case power consumption under different numbers of switching stage in a link, with optimal λ_{MR_0} and thermal tuning, $2\delta = 3.1nm$

switching stages in an ONoC architecture and the bandwidth of switching elements are also important factors affecting the power efficiency of ONoCs under temperature variations.

ACKNOWLEDGMENT

The authors are grateful to the reviewers who offer us helpful suggestions to improve this paper. This work is partially supported by RGC of the Hong Kong Special Administrative Region, China.

REFERENCES

[1] W. Dally and B. Towles, "Route packets, not wires: on-chip interconnection networks," in *Proc. Design Automation Conf.*, 2001, pp. 684–689.

[2] J. Xu, W. Wolf, J. Henkel, and S. Chakradhar, "H. 264 HDTV decoder using application-specific networks-on-chip," in *Multimedia and Expo. IEEE International Conference on*, July 2005, pp. 1508–1511.

[3] I. Young, E. Mohammed, J. Liao, A. Kern, S. Palermo, B. Block, M. Reshotko, and P. Chang, "Optical I/O technology for tera-scale computing," in *IEEE Int. Solid-State Circuits Conf.*, 2009, pp. 468–469.

[4] N. Kirman, M. Kirman, R. Dokania, J. Martinez, A. Apsel, M. Watkins, and D. Albonesi, "On-chip optical technology in future bus-based multicore designs," *IEEE Micro*, vol. 27, no. 1, pp. 56–66, Jan.-Feb. 2007.

[5] K. H. Mo, Y. Ye, X. Wu, W. Zhang, W. Liu, and J. Xu, "A hierarchical hybrid optical-electronic network-on-chip," in *VLSI (ISVLSI), 2010 IEEE Computer Society Annual Symposium on*, July 2010, pp. 327–332.

[6] M. Briere, B. Girodias, Y. Bouchebaba, G. Nicolescu, F. Mieyeville, F. Gaffiot, and I. O'Connor, "System level assessment of an optical NoC in an MPSoC platform," in *Design, Automation Test in Europe Conf. and Exhibition*, 2007, pp. 1–6.

[7] A. Shacham, K. Bergman, and L. Carloni, "On the design of a photonic network-on-chip," in *First Int. Symp. Networks-on-Chip*, 2007, pp. 53–64.

[8] H. Gu, J. Xu, and W. Zhang, "A low-power fat tree-based optical network-on-chip for multiprocessor system-on-chip," in *Design, Automation Test in Europe Conf. and Exhibition*, Apr. 2009, pp. 3–8.

[9] X. Wu, Y. Ye, W. Zhang, W. Liu, M. Nikdast, X. Wang, and J. Xu, "Union: A unified inter/intra-chip optical network for chip multiprocessors," in *Nanoscale Architectures (NANOARCH), 2010 IEEE/ACM International Symposium on*, June 2010, pp. 35–40.

[10] K. Skadron, M. R. Stan, K. Sankaranarayanan, W. Huang, S. Velusamy, and D. Tarjan, "Temperature-aware microarchitecture: Modeling and implementation," *ACM Trans. Archit. Code Optim.*, vol. 1, no. 1, pp. 94–125, 2004.

[11] A. Syrbu, A. Mereuta, V. Iakovlev, A. Caliman, P. Royo, and E. Kapon, "10 Gbps VCSELs with high single mode output in 1310nm and 1550 nm wavelength bands," in *Conf. Optical Fiber communication/National Fiber Optic Engineers*, 2008, pp. 1–3.

[12] H. Gu, J. Xu, and Z. Wang, "ODOR: a microresonator-based high-performance low-cost router for optical networks-on-chip," in *Proceedings of the 6th IEEE/ACM/IFIP international conference on Hardware/Software codesign and system synthesis*, ser. CODES+ISSS '08. New York, NY, USA: ACM, 2008, pp. 203–208.

[13] H. Gu, K. H. Mo, J. Xu, and W. Zhang, "A low-power low-cost optical router for optical networks-on-chip in multiprocessor systems-on-chip," in *VLSI. IEEE Computer Society Annual Symposium on*, May 2009, pp. 19–24.

[14] H. Gu, J. Xu, and Z. Wang, "A novel optical mesh network-on-chip for gigascale systems-on-chip," in *Circuits and Systems. IEEE Asia Pacific Conference on*, Dec. 2008, pp. 1728–1731.

[15] Y. Pan, P. Kumar, J. Kim, G. Memik, Y. Zhang, and A. Choudhary, "Firefly: Illuminating future network-on-chip with nanophotonics," in *Proc. 36th Int. Symp. Computer Architecture (ISCA)*, 2009.

[16] W. Huang, "Hotspot: A chip and package compact thermal modeling methodology for VLSI design," *PhD dissertation, Electrical and Computer Engineering, University of Virginia*, 2007.

[17] F. Magno, F. DellOlio, and V. M. N. Passaro, "Multiphysics investigation of thermo-optic effect in silicon-on-insulator waveguide arrays," in *Proc. COMSOL Users Conf.*, 2006.

[18] R. Michalzik and K. J. Ebeling, "Operating principles of VCSELs," *University of Ulm, Optoelectronics Department, Germany*.

[19] S. Mogg, N. Chitica, U. Christiansson, R. Schatz, P. Sundgren, C. Asplund, and M. Hammar, "Temperature sensitivity of the threshold current of long-wavelength InGaAs-GaAs VCSELs with large gain-cavity detuning," *IEEE J. Quantum Electronics*, vol. 40, no. 5, pp. 453–462, May. 2004.

[20] C. Chen, P. Leisher, A. Allerman, K. Geib, and K. Choquette, "Temperature analysis of threshold current in infrared vertical-cavity surface-emitting lasers," *IEEE J. Quantum Electronics*, vol. 42, no. 10, pp. 1078–1083, Oct. 2006.

[21] R. Amatya, C. Holzwarth, M. Popovic, F. Gan, H. Smith, F. Kartner, and R. Ram, "Low power thermal tuning of second-order microring resonators," in *Conf. Lasers and Electro-Optics*, May. 2007, pp. 1–2.

[22] T. Baehr-Jones, M. Hochberg, C. Walker, E. Chan, D. Koshinz, W. Krug, and A. Scherer, "Analysis of the tuning sensitivity of silicon-on-insulator optical ring resonators," *J. Lightwave Technology*, vol. 23, no. 12, pp. 4215–4221, Dec. 2005.

[23] S. Xiao, M. H. Khan, H. Shen, and M. Qi, "Compact silicon microring resonators with ultra-low propagation loss in the C band," *Opt. Express*, vol. 15, no. 22, pp. 14 467–14 475, 2007.

[24] B. G. Lee, B. A. Small, K. Bergman, Q. Xu, and M. Lipson, "Transmission of high-data-rate optical signals through a micrometer-scale silicon ring resonator," *Opt. Lett.*, vol. 31, no. 18, pp. 2701–2703, 2006.

[25] S. Xiao, M. H. Khan, H. Shen, and M. Qi, "Modeling and measurement of losses in silicon-on-insulator resonators and bends," *Opt. Express*, vol. 15, no. 17, pp. 10 553–10 561, 2007.

[26] S. Xiao, M. H. Khan, H. Shen, and M. Qi, "Multiple-channel silicon micro-resonator based filters for WDM applications," *Opt. Express*, vol. 15, no. 12, pp. 7489–7498, 2007.

[27] F. A. Xia, L. A. Sekaric, and Y. T. Vlasov, "Ultracompact optical buffers on a silicon chip," *Nature Photonics*, no. 1, pp. 65–71, 2007.

[28] Y. Vlasov and S. McNab, "Losses in single-mode silicon-on-insulator strip waveguides and bends," *Opt. Express*, vol. 12, no. 8, pp. 1622–1631, 2004.

[29] G. Masini, G. Capellini, J. Witzens, and C. Gunn, "A 1550nm, 10Gbps monolithic optical receiver in 130nm CMOS with integrated Ge waveguide photodetector," in *4th IEEE Int. Conf. Group IV Photonics*, 2007, pp. 1–3.

[30] S. Koester, L. Schares, C. Schow, G. Dehlinger, and R. John, "Temperature-dependent analysis of Ge-on-SOI photodetectors and receivers," in *3rd IEEE Int. Conf. Group IV Photonics*, 2006, pp. 179–181.

[31] M. Morse, O. Dosunmu, G. Sarid, and Y. Chetrit, "Performance of Ge-on-Si p-i-n photodetectors for standard receiver modules," *IEEE Photonics Technology Letters*, vol. 18, no. 23, pp. 2442–2444, Dec. 2006.

[32] F. Gan, T. Barwicz, M. Popovic, M. Dahlem, C. Holzwarth, P. Rakich, H. Smith, E. Ippen, and F. Kartner, "Maximizing the thermo-optic tuning range of silicon photonic structures," in *Photonics in Switching*, Aug. 2007, pp. 67–68.